MINISTRY OF EDUCATION AND TRAINING MINISTRY OF TRANSPORT
UNIVERSITY OF TRANSPORT TECHNOLOGY

HOANG THI HUONG GIANG

INVESTIGATION OF GRAPHENE OXIDE FOR ENHANCING THE MECHANICAL PROPERTIES OF ASPHALT CONCRETE UNDER VIETNAMESE CONDITIONS

Field of study: Transportation Construction Engineering
Code: 9580205

SUMMARY OF DOCTORAL THESIS

HA NOI – 2023

This research is completed at:
University of Transport Technology

Supervisors::

1. AssocProf.Dr. Nguyen Hoang Long
University of Transport Technology

2. Dr. Ly Hai Bang
University of Transport Technology

Reviewer 1:
Reviewer 2:
Reviewer 3:

The thesis will be defended before Doctoral–Level Evaluation Council at the University of Transport Technology
at …… on …… th ……. 2023

The thesis can be read at:
- National Library of Vietnam
- Library of the University of Transport Technology

INTRODUCTION

I. Research background

Due to its advantages, asphalt concrete (AC) is a widely used and important material in road construction globally. The quality of AC largely depends on the binding agent. In Vietnam, the reliance on foreign markets for asphalt imports presents challenges in maintaining quality control. While the adoption of asphalt 60/70 has been common in the country, it has shown certain limitations in its mechanical properties. Over the course of their service life, AC roads constructed with asphalt 60/70 frequently encounter issues like rutting and cracking due to the impact of vehicle loads and weather. These problems ultimately contribute to road deterioration. Therefore, improving the quality of AC road surfaces has been a subject of interest and research among scientists for many years.

To enhance the quality of AC, current global approaches encompass the incorporation of additives aimed at enhancing asphalt properties, fine-tuning the mix design to align with specific objectives, and the adoption of superior-quality materials. Furthermore, an ongoing avenue of exploration involves enhancing the AC mix through the integration of reinforcing materials. Among these, the utilization of asphalt additives to enhance the quality of AC has garnered considerable attention and is constantly evolving. Today, as scientific and engineering knowledge continues to advance, the utilization of nanotechnology and materials is gaining growing prominence in asphalt improvement. A notable recent emphasis has centered on graphene oxide (GO), a nano-material within the carbon family, which has shown promising outcomes. Nevertheless, it is important to note that a significant portion of these studies has been primarily concentrated in technologically advanced countries, with China being a prominent example. In Vietnam, GO is a relatively novel material that necessitates thorough research for gradual integration, ultimately contributing to the improvement of construction and road maintenance quality. Consequently, the thesis titled "Investigation of Graphene Oxide for Enhancing the Mechanical Properties of Asphalt Concrete under Vietnamese Conditions" is both well-timed and carries substantial scientific and practical importance.

II. Objective of the research

- Investigating the morphology, chemical composition, and mechanical properties of GO-modified asphalt (N_GO) to propose an optimal GO content in AC;
- Design the AC using GO (BTN_GO); comparative evaluation of BTN_GO with control AC based on various mechanical properties;
- Application of machine learning model to predict mechanical properties of N_GO and BTN_GO, application of BTN_GO in soft pavement structure for some automobile roads in Vietnam

III. Object and scope of the research

- The research object is asphalt 60/70 with GO and tight asphalt concrete with the nominal maximum particle size of 12.5 mm (BTNC 12.5) using GO additive; control materials are asphalt 60/70 and BTNC 12.5 without GO;
- The scope of the research includes experimental research in the laboratory; evaluating the effect of one type of GO on one type of asphalt, and one type of

aggregate; researching the behavior of BTN_GO when used as the surface layer of soft pavement on some high-level roads in Vietnam.

IV. Scientific and practical contribution

- Analyze and clarify the scientific basis for using GO in BTN. Composition and structure analysis of N_GO and BTN_GO. Analyze the advantages, disadvantages, and scope of application of this new material with Vietnamese conditions;
- Propose a reasonable ratio of GO in the mixture, material requirements, physical and mechanical criteria, and design method for BTN_GO in Vietnam;
- Determine the technical criteria of BTN_GO when designing pavement structures according to TCCS 38:2022/TCDBVN standards and mechanical-experimental methods (M-E);
- Applying machine learning models to build a tool to quickly predict some physical and mechanical properties of N_GO and BTN_GO;
- Proposing some high-level flexible pavement structures using the BTN_GO layer.

CHAPTER 1. LITERATURE REVIEW

1.1. Review of nanomaterials

Nanomaterials are materials that must have at least one dimension at the nanometer scale in their structure. They come in various forms, such as particles, fibers, sheets, plates, or tubes. Nanomaterials exhibit unique properties that traditional materials lack due to their reduced size and increased surface area. Over the past decade, with the rapid development of nanotechnology, nanomaterials are increasingly being utilized in improving asphalt, such as nano clay minerals, nano metals (ZnO, Al_2O_3, Fe_2O_3), nanofibers, nano-silica, and carbon nanotubes.

GO is a nanomaterial belonging to the carbon family, known for about 150 years. Research on the use of GO in asphalt improvement has only emerged in recent years, with a relatively modest number of studies conducted. Therefore, the application of GO to enhance asphalt is still a relatively new and promising research direction.

1.2. Review of graphene oxide

1.2.1. Origin of graphene oxide

GO originates from graphite (carbon), with its main constituent being carbon. Carbon is the most versatile element in the periodic table of chemical elements. These atoms have the ability to form various types of bonds not only with themselves but also with many other atoms, such as hydrogen, oxygen, nitrogen, and sulfur. Carbon atoms can bond with themselves through single, double, or triple bonds, forming various types of chains, rings, and three-dimensional (3D)

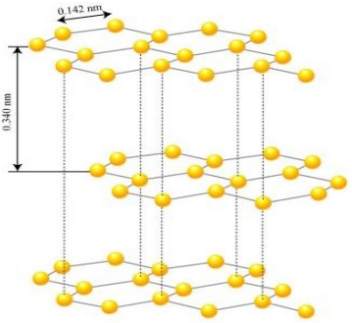

Figure 1.1. Structure of graphite.

structures. Therefore, graphite has a layered structure, with layers held together by Van der Waals forces at a distance of approximately 0.34 nm (Figure 1.1).

1.2.2. Structure of graphene oxide

With its single-atom layered structure, GO possesses multiple surface polar functional groups, with at least four identified groups, including hydroxyl (C-OH), epoxy (C-O-C), carboxylic (COOH), and carbonyl (C=O) groups (Figure 1.3). These functional groups enhance the reactivity of GO while simultaneously increasing the interlayer spacing between GO layers.

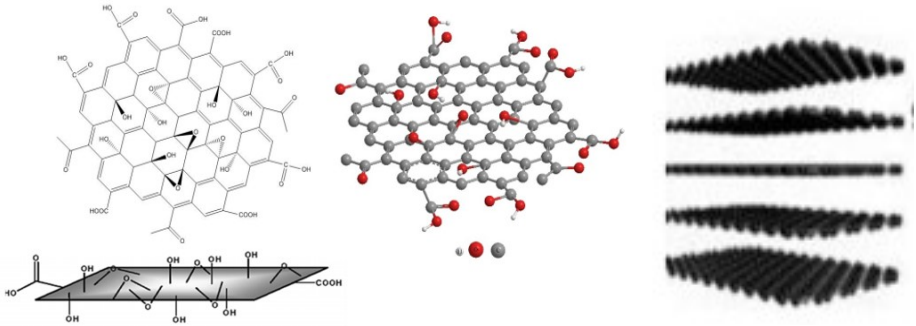

(a) GO 2D (b) GO 3D (c) Layers of GO

Figure 1.3. The chemical structure of GO.

1.2.3. Properties of graphene oxide

– Hygroscopic properties;

– Dispersibility;

– Covalent and non-covalent.

1.2.4. Methods of modulation graphene oxide

GO is produced by treating graphite with strong oxidizing agents such as HNO_3, H_2SO_4, $KMnO_4$, H_3PO_4, and $KClO_3$. The oxidation of graphite into GO can be achieved through various methods, including the Brodie (1859), Staudenmaier (1898), Offenman(1937), Hummers (1958), modified Hummers and Tour (2010), and electrochemical methods.

1.2.5. Types of graphene oxide

The global market offers types of GO, which can be categorized into 2 main types:

- Type 1: Laboratory-synthesized GO. This type of GO is typically in the form of a solution, solid, or powder, with a few layers of structure and an extremely high surface area, reaching up to 2600 m^2/g, and a purity level of up to 99%.
- Type 2: Industrially produced GO. This type of GO is often in the form of black or brown powder, with a structure consisting of 5-10 layers, a surface area ranging from 50-450 m^2/g, and a purity level ≥ 95%.

1.3. Mechanism of interaction between graphene oxide and asphalt

The mechanism of interaction between GO and asphalt is a complex and ongoing research topic. However, some studies have indicated that GO can interact with asphalt

molecules through various mechanisms, including Van der Waals interactions, electrostatic interactions, and chemical interactions.

1.4. Review of research on asphalt and asphalt concrete using graphene oxide in the world and Vietnam

1.4.1. Researches of asphalt using graphene oxide in the world

Research on using GO as an additive for asphalt has only started since 2015 and is still quite limited (about 20 studies). The studies mainly focus on Asian countries such as China (10-15 studies), Malaysia (2-3 studies), and India (2-3 studies). Many types of asphalt (80/100, A70, A90, AC30, SBS, PG58-34), GO types (single layer, multilayer), and physical and mechanical properties of asphalt were evaluated. However, the studies still have some limitations such as (1) Lack of specific assessments on the effects of aging during the mixing of N_GO when the mixing parameters are quite high; (2) The temperature-viscosity relationship of N_GO has not been established to determine the mixing and compaction temperature range of the BTN_GO mixture; (3) The number of indicators in each study is limited, so the assessment of the impact of GO on asphalt is not complete.

1.4.2. Research of asphalt concrete using graphene oxide in the world

The research on AC using GO in the world started in 2019 with about 5-7 studies. The studies only focused on AC 13,2 and AC 9,5 (graded according to Chinese standards JTG F40-2004).

In general, the research on AC using GO has some limitations. Firstly, the number of research indicators is not much, many important indicators of asphalt concrete have not been evaluated, such as rutting resistance in a water environment and cracking resistance through cracking tolerance index (CTindex), dynamic module, etc. Second, these studies mainly focus on some Asian countries, especially China, where the temperate monsoon climate is different from the tropical one with abundant rainfall and high humidity like Vietnam. Third, there has been no research on AC 12,5, which is the common type used as the top layer in soft pavement texture in Vietnam. Finally, the new studies focus on laboratory experiments without analyzing the behavior of BTN_GO as the surface layer in soft pavement texture to confirm the working ability of this material.

1.4.3. Research on asphalt and asphalt concrete using graphene oxide in Vietnam

Currently, Vietnam has no research on GO in the field of pavement construction in general and AC pavement in particular.

1.5. Research using machine learning to predict characteristics of asphalt and AC

In recent years, with the robust development of Industry 4.0 technology, along with its attributes of simplicity, automation, efficiency, and high applicability, many studies have been focused on the utilization of Machine Learning (ML) based on experimental test results. This technique is becoming increasingly popular and is being applied in numerous fields, including flexible pavement:

- Predict physical and mechanical properties of asphalt using additives;
- Predict mechanical properties of AC such as Marshall parameters, dynamic modulus, rutting resistance, and fatigue life;

- Predict operating criteria of AC pavement such as cracks, potholes, and IRI.

1.6. Identify the research issues of the thesis

- Proposed process for manufacturing N_GO adhesive from GO and 60/70 asphalt;
- Research the morphology, chemical composition, and physical and mechanical properties of N_GO, thereby determining the mixing and compaction temperature of BTN_GO;
- Research the mechanical properties of BTN_GO to serve the design of flexible pavement structures according to TCCS38:2022/TCDBVN and M-E methods. From there, evaluate the applicability of BTN_GO in the construction of AC pavement;
- Applying ML algorithms to construction tools to quickly and accurately predict some mechanical properties of N_GO and BTN_GO. This is useful for materials engineers, saving time and money in future research.

1.7. Research Methods

The thesis uses a combination of research methods: theoretical method, statistical probability method, experimental method, modeling method, and ML method.

CHAPTER 2. RESEARCH THE BASIC PROPERTIES OF ASPHALT USING GRAPHENE OXIDE

From the research objectives, research methods, and findings summarized in Chapter 1, Chapter 2 proceeds with experimental investigations on the morphology and chemical composition to determine the interaction between GO and asphalt; determine the basic properties of N_GO to select the appropriate GO content for use in AC, and to choose the mixing and compaction temperatures for the BTN_GO mixture. This chapter also includes control experiments to evaluate the advantages and disadvantages of N_GO compared to the commonly used asphalt 60/70 in Vietnam.

2.1. Determine the composition and manufacture of asphalt using graphene oxide

2.1.1. Selection of asphalt used in the research

Research using asphalt 60/70, provided by Petrolimex Asphalt Company Limited.

2.1.2. The type and content of graphene oxide

The GO used in the research is multilayer GO (5-10 layers) provided by Tandem Graphene Company, Suzhou, China, in powder form and black. The GO content selected is 0.5%, 1%, 1.5%, 2%, and 3% according to the asphalt mass.

2.1.3. Mixing temperature, mixing time, and mixing speed

Based on the general research, laboratory conditions, and type of asphalt, the study selected mixing parameters when adding GO to asphalt as follows: Mixing time of 20 minutes; mixing speed of 2000 rpm, mixing temperature 150^{o}C

2.2. Experimental research on the morphology and chemical composition of N_GO

2.2.1. Methods of analyzing the morphology and chemical structure of materials

- Infrared spectroscopy determines chemical structure;

– Scanning electron microscope determines material morphology

2.2.2. Experiment plan

In this section, the morphology and chemical composition of asphalt 60/70, GO, and N_GO are investigated. To observe the influence of GO on the morphology and chemical composition of asphalt, only GO content of 1%, 2%, and 3% are examined.

2.2.3. Experimental results

2.2.3.1. The results of SEM morphology analysis of the materials

The SEM image of GO (Figure 2.5) shows that the GO particles are primarily in an independent, multi-layered state. During the high-speed mixing and shearing process, the shearing force will break and separate GO from multi-layered to single-layered, increasing the surface area ratio, and making it easier to disperse into the asphalt.

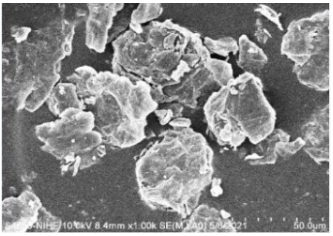

Figure 2.5. SEM image of GO.

SEM of N_GO (Figure 2.7) shows:

– 2% GO for uniform dispersion in asphalt

– GO content increased to 3%, GO dispersion in asphalt decreased

– GO content increases, and surface roughness improves.

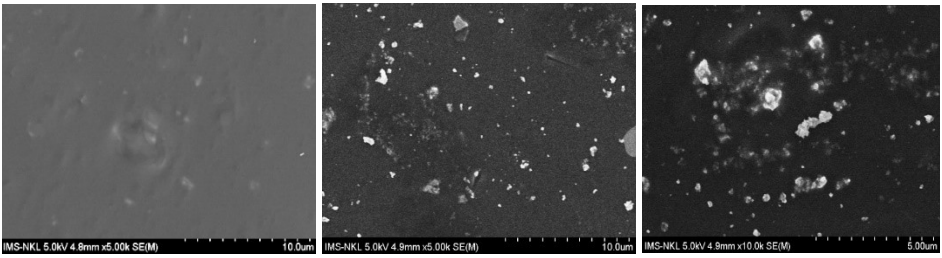

N_GO_1% N_GO_2% N_GO_3%

Figure 2.7. SEM image of N_GO.

2.2.3.2. Experimental results of chemical structure analysis of materials

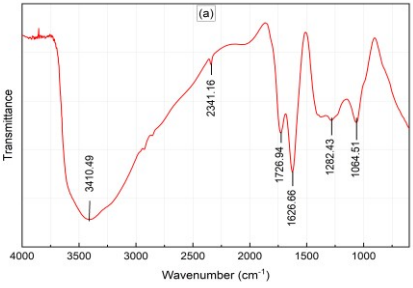

Figure 2.8. FTIR spectrum of GO.

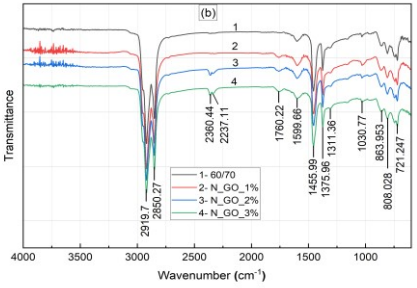

Figure 2.9. FTIR spectrum of N_GO.

The FTIR spectrum of GO in Figure 2.8 indicates the presence of oxygen functional groups that contribute to its strong hydrophilic nature. Therefore, GO is a stable material and may enhance the rheological properties of the asphalt. Figure 2.9 shows the development of a new peak at a wavelength of 1760,22 cm^{-1} in the N_GO samples, which could be a sign of a reaction occurring between GO and asphalt 60/70.

2.3. Experimental research on the basic properties of asphalt using graphene oxide

2.3.1. Experimental criteria

The thesis conducts experiments on several basic criteria and other parameters as stipulated by the TCVN 7493:2005 standard for N_GO with five different GO content levels: 0.5%, 1%, 1.5%, 2%, and 3%. The control material is asphalt 60/70 without GO (C01). Additionally, to evaluate the influence of aging during the production of N_GO binding material, the study also uses another control material (C02), which is asphalt 60/70 mixed with a specific time, speed, and temperature parameters similar to the N_GO samples for penetration and softening point criteria.

2.3.2. Results of the penetration test

The penetration test is conducted according to TCVN 7495:2005. The evaluation of the test result's precision followed ASTM C670 standards, with acceptable limits specified by TCVN 7495:2005. The test results ensure compliance with the precision standards. Using Minitab 19 software, a Design of Experiments is designed using the General Full Factorial method. The ANOVA variance analysis is performed at a significance level of $\alpha = 0.05$, and post hoc analysis using the Tukey method was conducted to detect pairwise differences. The ANOVA analysis results, with a p-value << 0.05, and an adjustment determination coefficient R^2_{dc} = 90.83%, indicating that the GO content significantly affects penetration at a high level of statistical confidence

Figure 2.13 shows the effect of GO contents on the penetration of asphalt:

- The penetration of the C02 is slightly lower than that of C01 due to the aging effect during mixing, but this influence is not significant.
- The penetration of N_GO decreases as the GO content increases and is lower than that of asphalt 60/70, indicating that GO increases the stiffness of the asphalt.

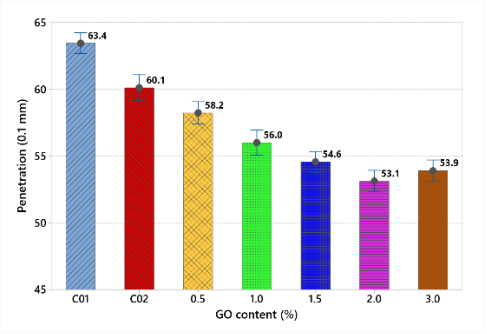

Figure 2.13. Penetration of N_GO.

- N_GO_2% has the lowest penetration (53.1), demonstrating better improvement compared to other GO content levels.

2.3.3. Results of softening point test

The softening point of the asphalt is determined according to TCVN 7497-2005 standards. The precision of the test results is evaluated according to ASTM C670 standards, with acceptable limits specified by TCVN 7497:2005. The precision analysis

shows that the test results meet the evaluation standards. Figure 2.15 presents the softening point test results of N_GO at different GO content levels. It is easily noticeable that the softening point increases as the GO content increases and is higher than that of the control samples. N_GO_2% has the highest softening point at 53.6°C. The softening point of N_GO_3% is lower than that of N_GO_2%, confirming the better dispersibility of N_GO_2%. Therefore, adding GO beyond the optimal content will reduce the performance improvement of the asphalt.

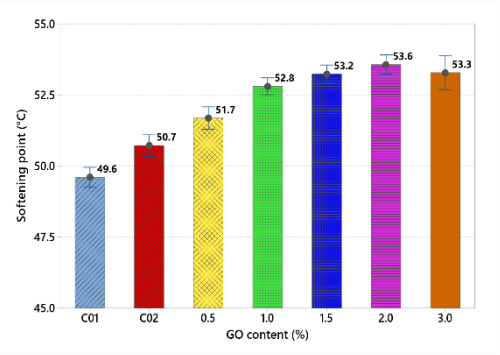

Figure 2.15. Softening point of N_GO.

2.3.4. Results of the viscosity test

In this study, a Brookfield viscometer is used to measure asphalt viscosity at three temperatures from low to high: 135ºC, 155ºC, and 175ºC. Experimental standards for determining viscosity using a Brookfield viscometer according to TCVN 11196:2017. Brookfield viscosity test results ensure precision according to evaluation standards.

The effect of GO on the viscosity of N_GO at temperatures from 135ºC to 175ºC is shown in Figure 2.18. Some observations are made:

– Viscosity decreases as temperature increases
– Viscosity increases as GO content increases.

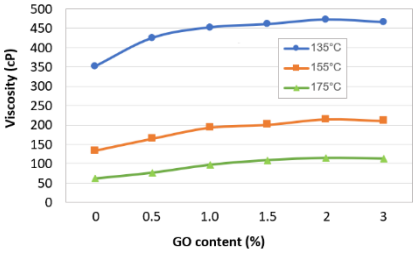

Figure 2.18. Viscosity of N_GO at temperatures

N_GO_2% has the highest viscosity at all temperatures, and is 34.76% higher; 60.45%, and 88.52% compared to 60/70 asphalt at 135ºC, 155ºC, and 175ºC.

The regression equation for the relationship between the viscosity of N_GO with the GO content and testing temperature (T) within the study limits is as follows:

$$\mathbf{Viscosity = 1535 + 25,67xGO - 8,576xT\ (cP)} \qquad (2.1)$$

From formula (2.1), determine the mixing and compaction temperature range of asphalt types according to ASTM 2493 standard, corresponding to the viscosity range of 170 ± 20 cP and 280 ± 30 cP. The results of determining the temperature range of mixing and compaction of BTN_GO are presented in Table 2.5.

Table 2.5. Range of mixing and compaction temperature of BTN_GO.

Temperature Range (ºC)	N_GO binders					
	60/70 asphalt	N_GO_0,5%	N_GO_1%	N_GO_1,5%	N_GO_2%	N_GO_3%
Mixing	148 ÷ 152	152 ÷ 155	154 ÷ 158	155 ÷ 159	156 ÷ 160	156 ÷ 160
Compaction	137 ÷ 142	142 ÷ 147	144 ÷ 149	145 ÷ 150	146 ÷ 151	146 ÷ 151

In general, GO increases the mixing and compaction temperature of BTN_GO mixture compared to BTNC 12.5 from 5÷8ºC. The addition of additives such as Sasobit and WCO may reduce the mixing and compaction temperature of the BTN_GO mixture.

2.3.5. Dynamic shear rheometer

The dynamic shear rheometer test of N_GO is conducted according to AASHTO T315 standards and ensures precision.

Figure 2.20 shows that as GO content increases, G*/sinδ increases, indicating better resistance to rutting in high-temperature environments for N_GO compared to asphalt 60/70. N_GO_2% and N_GO_3% binders exhibit performance characteristics equivalent to PG70, while other N_GO types are equivalent to PG64.

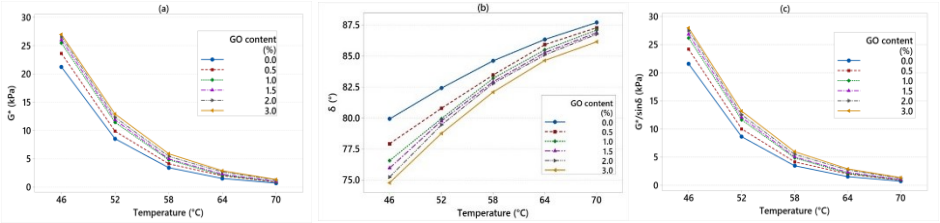

Figure 2.20. Dynamic shear modulus (a), phase angle (b), and G*/sinδ (c) of unaged N_GO.

The regression equation for the relationship between the G*/sinδ of N_GO with the GO (0 – 3%) content and testing temperature (T) within the study limits is as follows:

$$\mathbf{G^*/\sin\delta = 64{,}3 + 0{,}99xGO - 0{,}9758xT\ (kPa)} \quad (2.2)$$

The equation ensures reliability with R^2_{dc}= 85%, p << 0.05

The dynamic shear modulus tests of the binders after RTFOT aging are conducted. Several conclusions were drawn:

– PG of N_GO after RTFO remains the same as the original N_GO asphalt.
– The change G*/sinδ of N_GO is smaller compared to 60/70 asphalt, which shows GO not only improves the high-temperature stability of the asphalt but also reduces the impact of the aging process on its rheological properties.

2.3.6. Experiment on basic properties of N_GO

Experimental results of other basic properties of N_GO are presented in Table 2.7.

Table 2.7. Experimental results of some remaining properties of N_GO.

Properties	Standards	N_GO binders						Limit
		0%	0,5%	1%	1,5%	2%	3%	
Ductility at 25ºC, cm	TCVN 7496:2005	140	131	121	115	108	102	Min 100
Flash-point, ºC	TCVN 7498:2005	310	301	295	291	287	280	Min 232
Coating criteria (Boiling method)	TCVN 7504:2005	Grade 3	Grade 3	Grade 3	Grade 4	Grade 4	Grade 4	Grade 3
Specific Gravity, g/cm^3	TCVN 7501:2005	1,032	1,032	1,032	1,032	1,032	1,032	1,00-1,05
Loss on heating at 163ºC for 5 hours	ASTM D1754	0,250	0,245	0,241	0,235	0,231	0,230	Max 0,8

Experimental results show that the properties of N_GO binders meet the requirements according to TCVN 7493:2005 standard. Significantly, the addition of GO increases the adhesion to aggregate for N_GO_1.5%, N_GO_2%, and N_GO_3% binders from level 3 to level 4. This result shows that GO may enhance the bonding ability between the asphalt and the aggregates, suggesting that GO reduces the moisture sensitivity of BTN_GO.

2.4. Conclusion for Chapter 2

- The high-speed mixing process will break down the GO into individual layers, facilitating a good dispersion in the asphalt. The optimal dispersion in the asphalt is achieved with a 2% GO content.
- There are at least 4 oxygen-containing functional groups found on the surface of GO sheets. The development of the new peak at wavenumber 1760.22 cm^{-1} may be an indication of the reaction that has occurred between GO and 60/70 asphalt.
- The effect of the mixing process (aging during mixing) when adding GO to 60/70 asphalt at 150^{o}C for 20 minutes and 2000 rpm is negligible.
- The addition of GO will increase the mixing and compaction temperature of the BTN_GO mixture compared to the control AC by 5 - 8^{o}C.
- GO improves the high-temperature performance of asphalt. The performance properties of N_GO_2% and N_GO_3% unaged and after RTFOT aging are equivalent to PG70, with the remaining GO content equivalent to PG64. GO reduces the impact of the aging process on the rheological properties of asphalt.
- GO increases the adhesion to aggregates of the binder from grade 3 to grade 4 at GO contents of 1.5%, 2%, and 3%. This suggests that GO reduces the moisture sensitivity of BTN_GO.

CHAPTER 3. EXPERIMENTAL RESEARCH ON MECHANICAL AND PHYSICAL PROPERTIES OF ASPHALT CONCRETE USING GRAPHENE OXIDE

From the results of the study of the basic properties of N_GO in Chapter 2, Chapter 3 focuses on researching the following contents: (1) Propose a method for designing the composition of BTN_GO mixture; (2) Experimental research on physical and mechanical properties of BTN_GO including Marshall stability and flow, static elastic modulus, splitting tensile strength, rutting resistance, cracking resistance, and dynamic module; (3) Construct the master dynamic modulus curves and model the master dynamic modulus curve of BTN_GO to determine the dynamic modulus at any temperature and frequency.

3.1. Design the composition of the asphalt concrete mixture using graphene oxide

- Design method: Marshall;
- Type of AC: BTNC 12.5;
- Aggregate: Sunway quarry, Quoc Oai, Hanoi;
- Mineral powder: Kien Khe quarry, Ha Nam;

– Based on the research results in Chapter 2, the optimal GO content for improving asphalt is found to be 2%. Therefore, this is the highest content used for testing BTN_GO. Furthermore, GO is a new additive in AC, to provide a more accurate assessment, the study conducted tests for the BTN_GO mixture with N_GO_1% and N_GO_1.5% as binders;

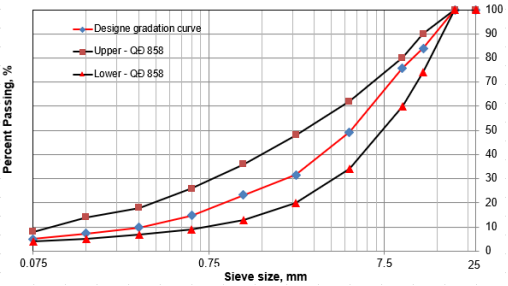

Figure 3.2. Design Aggregate Gradation Curve.

– Based on Table 2.5, the study selected mixing and compaction temperatures for the BTN_60/70 mixture as 150°C and 140°C, respectively, while for BTN_GO, these values are 155°C and 145°C, respectively.
– The optimal binder content for BTN_60/70 and BTN_GO is chosen as 4.6%, with V_a falling within the range of 4.5 to 5%, which is the recommended value according to decision 858/QĐ-BGTVT.

3.2. The selection of properties in the study

(1) The criteria for evaluating AC as required by Decision 858 include::

– Marshall stability and flow;
– Residual stability;
– Rutting resistance.

(2) The criteria serve for the design of flexible pavement structure according to TCCS 38:2022/TCĐBVN and the mechanical-experimental method:

– The static elastic modulus of BTN_GO at 3 temperatures.: 15°C, 30°C và 60°C;
– The tensile splitting strength of BTN_GO at 15°C (indirectly determined tensile strength through the formula);
– The dynamic modulus BTN_GO.

(3) Studying crack resistance through the crack resistance index.

3.3. Marshall stability, flow, and residual stability

3.3.1. Marshall stability and flow

The results of stability and Marshall flow tests are evaluated for precision according to ASTM D6927.

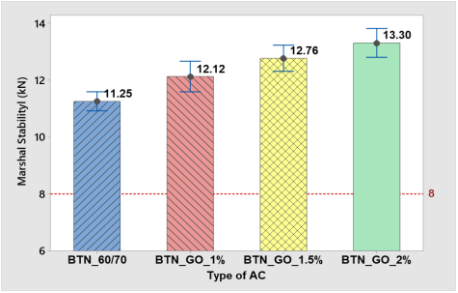

Figure 3.4. Marshall stability of BTN_GO.

The experimental results show that the Marshall stability (MS) of all types of AC is greater than 8.0 kN. BTN_GO exhibits increased MS compared to BTN_60/70, the higher the GO content, the greater the increase. BTN_GO_2% shows the highest MS, with an increase of 18.22% compared to

BTN_60/70 (Figure 3.4). This is attributed to GO enhancing the stiffness of the binder, leading to improved MS in BTN_GO. As the GO content increases, the stiffness of the binder also increases, resulting in higher MS.

The regression equation for the relationship between the MS with the GO content (0 – 2%) within the study limits is as follows:

$$\mathbf{MS = 11,2 + 1,03xGO\ (kN)} \quad (3.1)$$

Figure 3.5 is a summary chart of Marshall flow values based on GO content. The flow values for all samples fall within the specified range according to decision 858/QĐ-BGTVT (1.5÷4 mm). Additionally, the Marshall flow of BTN_GO_1%, BTN_GO_1.5%, and BTN_GO_2% decreases by 10.32%, 19.35%, and 28.06%, respectively, compared to BTN_60/70.

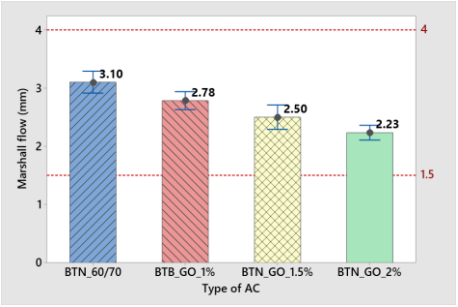

Figure 3.5. Marshall flow of BTN_GO.

3.3.2. Residual stability

The use of GO significantly enhances the remaining stability (RS) of BTN_GO. BTN_GO exhibits higher RS compared to BTN_60/70, with an increasing GO content leading to greater RS. BTN_GO_2% shows the highest RS with an RS of 92.33% (Figure 3.7). This indicates that the moisture resistance of BTN has been substantially improved after the incorporation of GO. The reason for this enhancement is attributed to the water molecules being adsorbed and tending to reside in the voids between the layers, creating a hydrogel network between water molecules and oxygen groups on GO, thereby reinforcing the water stability of BTN_GO.

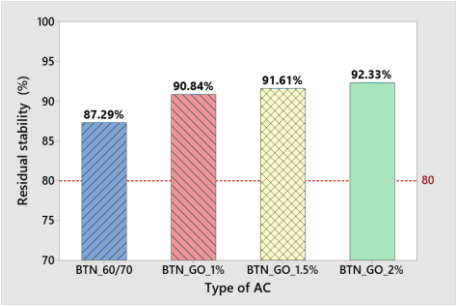

Figure 3.7. Residual stability of BTN_GO.

3.4. Resistance to rutting

In this study, the rutting resistance was conducted according to method A as specified in decision 1617/QĐ-BGTVT. The obtained results include the rutting depth in a water environment and the stripping point (if applicable). The rutting depth test results for BTN_60/70 and BTN_GO are detailed in Table 3.10 and Figure 3.

Table 3.10. The rutting resistance test results of BTN_60/70 and BTN_GO.

Nº	Information	Sample	BTN 60/70	BTN_GO 1%	BTN_GO 1,5%	BTN_GO 2%
1	The rutting depth, mm	Left	5,60	5,20	4,20	4,00
		Right	6,07	4,90	3,85	3,47
		Average	**5,84**	**5,05**	**4,03**	**3,74**

Nº	Information	Sample	BTN 60/70	BTN_GO 1%	BTN_GO 1,5%	BTN_GO 2%
2	Variation between results Rmax-min	mm	0,47	0,30	0,35	0,53
3	Permissible range, d2s	%	30	30	30	30
4	Permissible deviation: Average*(3)	mm	1,75	1,52	1,21	1,12
5	Evaluation: Comparing (2) and (4)	-	**Pass**	**Pass**	**Pass**	**Pass**

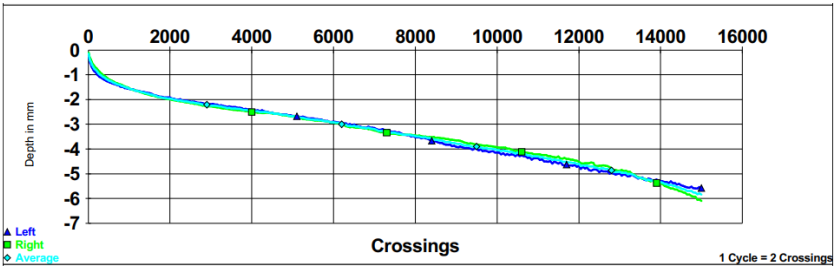

a. BTN_60/70.

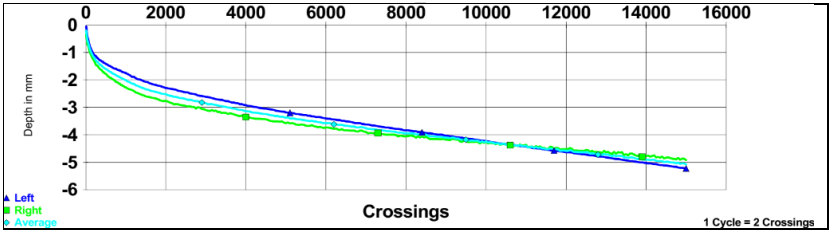

b. BTN_GO_1%.

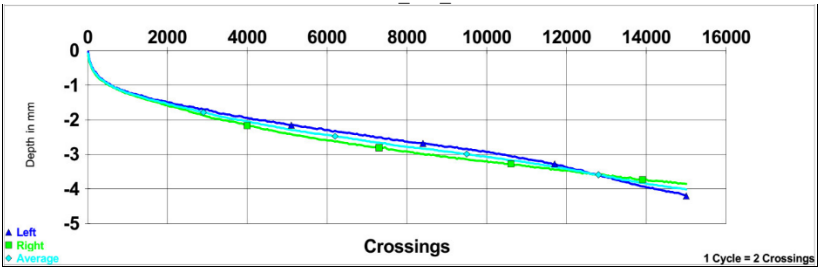

c. BTN_GO_1,5%.

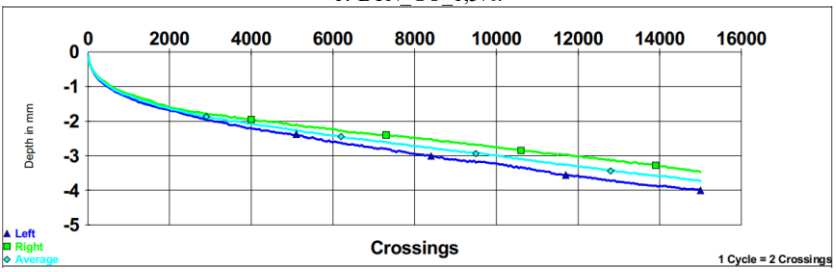

d. BTN_GO_2%.

Figure 3.9. Result of wheel tracking test.

The test results indicate that after 15,000 cycles in a water environment at 50°C, the rut depth of both BTN_60/70 and BTN_GO is less than the allowable value (12.5 mm) as required by decision 1617/QĐ-BGTVT. Furthermore, the permanent deformation of BTN essentially decreases significantly as the GO content increases. The use of 1%, 1.5%, and 2% GO by weight of the asphalt is effective in reducing rutting, with reductions of 13.53%, 30.99%, and 35.96%, respectively, compared to BTN_60/70. This demonstrates that the stiffening effect of GO on the binder has been improved, enhancing the high-temperature rutting resistance of BTN_GO.

3.5. Static elastic modulus

Static elastic modulus tests on BTN_60/70 and BTN_GO are conducted according to TCCS 38:2022/TCĐBVN standards. The test results ensure compliance with the precision standards.

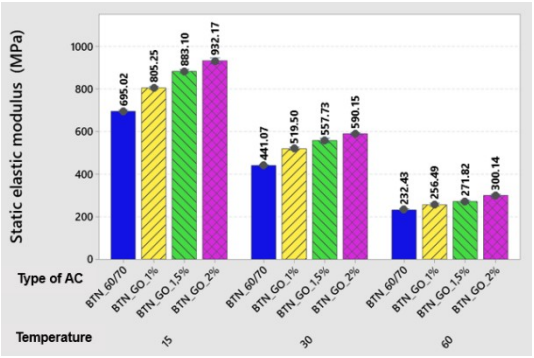

Figure 3.14. Static elastic modulus of BTN_GO.

The use of GO in BTN significantly increased the static elastic modulus at all three test temperatures. However, the influence of GO on the Static elastic modulus at 15°C is the most significant, followed by 30°C and finally 60°C. BTN_GO_2% exhibited the highest improvement in performance at all three temperatures compared to other GO content. Specifically, the static elastic modulus values for BTN_GO_2% increased by 34.12%, 33.80%, and 29.13% at temperatures of 15°C, 30°C, and 60°C, respectively, compared to BTN_60/70 (Figure 3.14).

The regression equation for the relationship between the static elastic modulus (E) with the GO content (0 – 2%) and testing temperature (T) within the study limits is as follows:

$$\mathbf{E = 836,9 + 106,86xGO - 210,48xT - 28,54xGOxT\ (MPa)} \quad (3.4)$$

3.6. Splitting tensile strength

The splitting tensile strength (R_{ke}) of BTN_GO is determined according to TCVN 8862:2011. The results (Figure 3.17) show that GO improves the splitting tensile strength at 15°C. Compared to BTN_60/70, the R_{ke} of BTN_GO_1%, BTN_GO_1.5%, and BTN_GO_2% increased by 13.55%, 19.84%, and 18.57%, respectively. This improvement may be attributed to the even dispersion of GO within the asphalt, enhancing the bond between aggregate particles and the N_GO binder. BTN_GO_1.5% exhibited the best performance in enhancing the splitting tensile strength compared to other GO content.

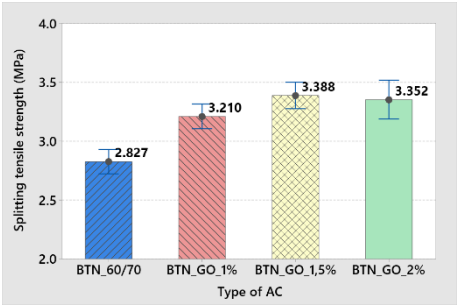

Figure 3.17. Splitting tensile strength of BTN_GO.

The regression equation for the relationship between the R_{ke} with the GO content (0 – 2%) within the study limits is as follows:

$$\mathbf{R_{ke} = 2{,}874 + 0{,}285xGO\ (kN)} \quad (3.8)$$

The flexural strength (R_{ku}) is approximately determined using the formula:: $R_{ku} = K_n . R_{ke}$ and is summarized in Table 3.14, with $K_n = 2$.

Table 3.14. Flexural strength of BTN_GO.

Types of AC	R_{ke}^{tb} (MPa)	R_{ku}^{tb} (MPa)
BTN_60/70	2.827	5.653
BTN_GO_1%	3.210	6.421
BTN_GO_1,5%	3.388	6.777
BTN_GO_2%	3.352	6.705

3.7. Cracking resistance

The cracking resistance of BTN_GO is conducted according to ASTM D8225-19 standards. The test results ensure compliance with the precision standards.

The test results are shown in Figure 3.22, indicating that the CT_{Index} values for BTN_60/70 and BTN_GO are both higher than the reference value from the Oklahoma Ballot ($CT_{Index} \geq 80$). Furthermore, the addition of GO does not improve the crack resistance of AC and tends to decrease the CT_{Index} slightly. Compared to BTN_60/70, the CT_{Index} values of BTN_GO_1%, BTN_GO_1.5%, and BTN_GO_2% decrease by 5.87%, 7.59%, and 8.61%, respectively. However, these are preliminary research results on BTNC_12.5 using asphalt 60/70. To provide a more comprehensive assessment, further studies on various types of AC and different asphalt are needed.

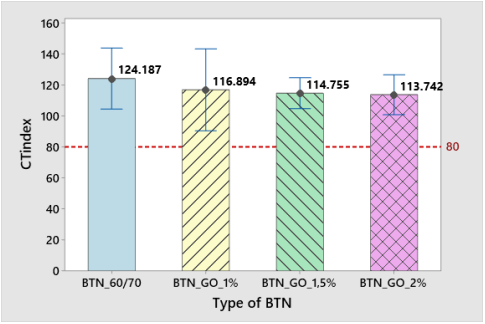

Figure 3.22. CT_{Index} of BTN_GO.

3.8. Dynamic modules

3.8.1. Experimental results and analysis

The tests are conducted at 4 temperatures: 4°C, 21°C, 37°C, and 54°C, with 6 frequency levels: 0.1 Hz, 0.5 Hz, 1 Hz, 5 Hz, 10 Hz, and 25 Hz. From the experimental results, several observations can be made:

- At the same frequency, as the temperature increases, |E*| decreases rapidly, while at the same temperature, as the frequency increases, |E*| increases. This explains the viscoelastic behavior of BTN_60/70 and BTN_GO;
- Under the same experimental conditions, the addition of GO increases |E*| of BTN_GO compared to BTN_60/70, and the higher the GO content, the larger |E*| becomes. However, this increase varies at different temperatures and test frequencies. At higher temperatures, the difference in |E*| values between BTN_GO and BTN_60/70 becomes more significant. Specifically, |E*| of BTN_GO_1% is approximately 1.03 – 1.08 times higher at 4°C and about 1.29 – 1.42 times higher at 54°C compared to BTN_60/70. Meanwhile, |E*| of BTN_GO_2% is approximately 1.09 – 1.16 times higher at 4°C and about 1.67 – 1.87 times higher at 54°C compared to BTN_60/70.

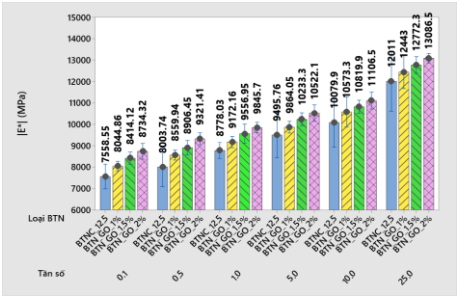

Figure 3.24. Chart |E*| of BTN_GO at 4ºC.

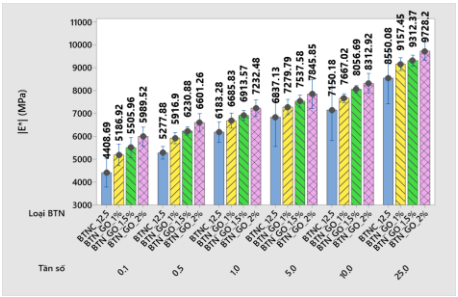

Figure 3.25. Chart |E*| of BTN_GO at 21ºC.

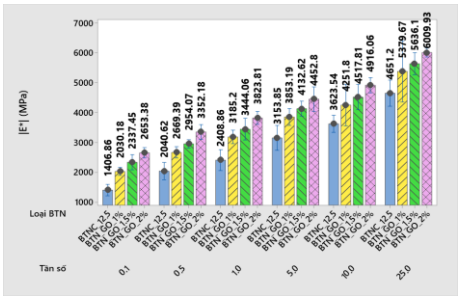

Figure 3.26. Chart |E*| of BTN_GO at 37ºC.

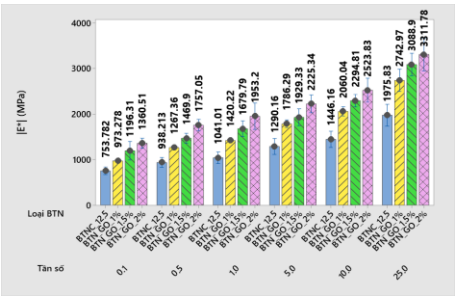

Figure 3.27. Chart |E*| of BTN_GO at 54ºC.

3.8.2. Establishing master curves of dynamic modulus

The |E*| master curve is a curve that represents the viscoelastic properties of AC over a wide range of frequencies and temperatures. This curve is constructed from the frequency-temperature shift rule, which is used to predict |E*| of AC at different frequencies and temperatures. The reference temperature chosen is 21°C. Isothermal curves corresponding to temperatures higher than 21°C will shift to the left, while curves corresponding to temperatures lower than 21°C will shift to the right through shift factors, a_T (Figure 3.29).

3.8.3. Modeling master curve of dynamic modulus

Simulating the experimental |E*| data of BTN_GO is carried out using the 2S2P1D model. This is a generalized model constructed by combining physical components, including 2 Springs, 2 Parabolic elements, and 1 Dashpot. The model employs 7 initial parameters to represent the linear viscoelastic properties of BTN_GO, as presented in Table 3.18. The modeling results for |E*| of various types of AC are depicted in Figure 3.32.

To assess the suitability of the 2S2P1D model with the experimental results, the study used the Goodness of Fit method. The results determined the coefficient of determination R^2 and S_e/S_y, as shown in Table 3.19. From the table results, it is evident that the 2S2P1D model is suitable for simulating the master curve |E*| of BTN_GO and the BTN_60/70.

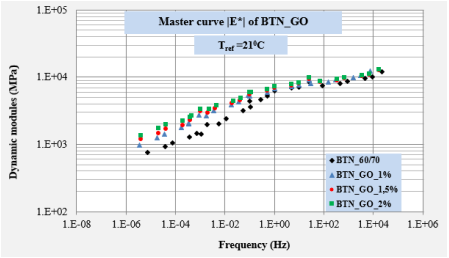

Figure 3.29. Master curve |E*| of BTN_GO.

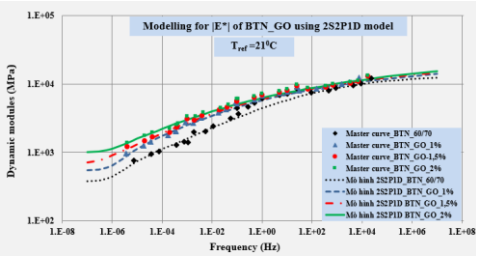

Figure 3.32. Modeling the master curve |E*| of BTN_GO according to the 2S2P1D model.

Table 3.18. Parameters of the 2S2P1D model simulate the master curve |E*|.

Type of BTN	E_{00} (MPa)	E_0 (MPa)	k	h	δ	τ (s)	β
BTN_60/70	380	19500	0,17	0,30	3,5	0,65	2000
BTN_GO_1%	550	27000	0,10	0,31	3,5	0,50	3000
BTN_GO_1,5%	700	30000	0,10	0,35	4,5	1,00	3500
BTN_GO_2%	1000	32000	0,10	0,35	5,0	1,00	2000

Table 3.19. Evaluate the forecast results |E*| of BTN_GO using the 2S2P1D model

Type of BTN	R^2	S_e/S_y	Assessment
BTN_60/70	0,9739	0,186	Very good
BTN_GO_1%	0,9910	0,110	Very good
BTN_GO_1,5%	0,9891	0,120	Very good
BTN_GO_2%	0,9876	0,128	Very good

3.9. Conclusions of Chapter 3

- The addition of GO increases the Marshall stability of BTN_GO compared to BTN_60/70, and the higher the GO content, the greater the increase. BTN_GO_2% exhibits the highest Marshall stability, with an increase of 18.22% compared to BTN_60/70. Additionally, GO also enhances the remaining stability of BTN_GO, with BTN_GO_2% having the highest remaining stability at RS = 92.33%, while BTN_60/70 has the lowest remaining stability at RS = 87.29%.
- GO significantly increases the static modulus of elasticity of BTN_GO compared to BTN_60/70 at all three test temperatures. BTN_GO_2% achieves the highest improvement in static modulus of elasticity at all three temperatures, with an increase ranging from 29.13% to 34.12% compared to BTN_60/70.
- The splitting tensile strength of BTN improves after the addition of GO. BTN_GO_1%, BTN_GO_1.5%, and BTN_GO_2% exhibit a respective increase in splitting tensile strength of 13.55%, 19.84%, and 18.57% compared to BTN_60/70.
- The rutting resistance of BTN_GO in a water environment is better than that of BTN_60/70. The rutting depth of BTN_GO_1%, BTN_GO_1.5%, and BTN_GO_2% decreases by 13.53%, 30.99%, and 35.96%, respectively, compared to BTN_60/70. This suggests an improvement in the pavement structure's performance when using BTN_GO as the surface layer based on rutting resistance.
- The crack resistance of BTN_GO is slightly lower compared to BTN_60/70 with the value CT_{index} decreasing by 5.87% to 8.61% as the GO content increases.
- The master curves of |E*| for BTN at the reference temperature of 21°C indicate that |E*| of BTN_GO is higher than that of BTN_60/70 at various temperatures and frequencies. |E*| of BTN_GO_2% achieves the highest value, followed by BTN_GO_1.5% and BTN_GO_1%, and BTN_60/70 has the lowest value.

– The 2S2P1D model is constructed to appropriately simulate the |E*| of BTN_GO and is used to determine the |E*|of BTN_GO at any temperature and frequency.

In summary, GO improves several physical properties of BTN, with BTN_GO_2% exhibiting superior physical characteristics compared to BTN_60/70, surpassing BTN_GO_1% and BTN_GO_1.5%. Therefore, BTN_GO_2% is selected for further investigation in the following chapter.

CHAPTER 4. STUDYING MATERIAL PHYSICAL PROPERTIES PREDICTION USING MACHINE LEARNING AND APPLICATION OF ASPHALT CONCRETE USING GO IN ROAD SURFACE STRUCTURES

Chapter 4 applies machine learning to develop a predictive tool for some physical properties of N_GO and BTN_GO, guiding future research. Additionally, several typical flexible pavement structures on national highways in Vietnam that originally used a BTNC_12.5 surface layer were selected. Subsequently, BTNC_12.5 is replaced with BTN_GO_2% at the designed thickness for analysis, comparison, and evaluation following TCCS 38:2022/TCĐBVN and the Mechanical-Experimental (M-E) method.

4.1. Machine learning application to predict properties of materials

4.1.1. Machine learning application to predict properties of asphalt using GO

With data collected from studies around the world and experimental data in Chapter 2, the research constructs datasets to predict properties including penetration, softening point, ductility, viscosity, and G*/sinδ. The input variables for these datasets are the GO content (X_1), the number of GO layers (X_2), the thickness of GO sheets (X_3), the average size of GO sheets (X_4), mixing temperature (X_5), mixing speed - RPM (X_6), mixing time (X_7), aging type (X_8), and the physical properties of the initial bitumen corresponding to each dataset (X_9). For the ductility, viscosity, and G*/sinδ datasets, there is an additional variable, the test temperature (X_{10}).

– The penetration dataset is constructed from 122 experimental data points from 11 studies. The study utilized an ANN algorithm and 10-fold cross-validation (CV) during the training, validation, and model testing process. After trial and error, the ANN model was trained using the traingdx algorithm with a 9-5-1 structure (ANN-GDX-9-5-1), which proved to be the best model for predicting the penetration of N_GO with $R^2 = 0.994$ (Figure 4.1).

– The softening point dataset is constructed from 130 experimental results from 11 studies. Using an ANN algorithm and a 10-fold CV technique, the ANN model with the structure of ANN-RP-9-10-1 is found to be the best model for predicting the softening point of N_GO with $R^2 = 0.996$ (Figure 4.2).

– The ductility dataset is constructed from 104 experimental results from 11 studies. The ANN model trained with the traingdx algorithm and having a structure of ANN-RP-10-9-1 is found to be the best model for predicting the ductility of N_GO with $R^2 = 0.999$ (Figure 4.3).

– The viscosity dataset is compiled from 164 experimental results from 7 studies. The ANN model with the structure of ANN-GDX-10-13-1 is found to be the best model for predicting the viscosity of N_GO with $R^2 = 0.983$ (Figure 4.4).

– The G*/sinδ dataset is constructed from 433 data points from 8 studies. The study employed the CGB algorithm and a 5-fold CV technique. The CGB model demonstrated high accuracy with r_s = 0.983 (Figure 4.5).

4.1.2. Machine learning application to predict Marshall stability of BTN_GO

The study used 11 input variables to predict the MS of BTN_GO, including the GO content (X_1), average number of GO layers (X_2), maximum number of GO layers (X_3), GO sheet thickness (X_4), and average diameter of GO sheets (X_5), initial asphalt penetration (X_6), optimum asphalt content (X_8), percentage of aggregate passing through sieve sizes 2.36 mm (X_9), passing through sieve 4.75 mm (X_{10}), passing through sieve 9.5 mm (X_{11}), and passing through sieve ≥ 12.5 mm (X_{12}). To predict the MS of BTN_GO, the study employed the CGB algorithm. Figure 4.6 illustrates the relationship between predicted and experimental MS values. It can be observed that the CGB model demonstrates high prediction accuracy with R = 0.975.

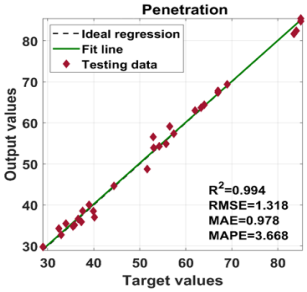

Figure 4.1. Regression graph of penetration dataset

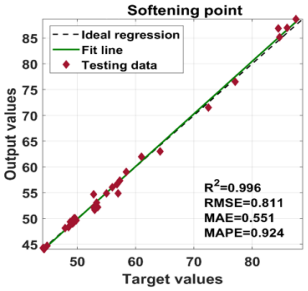

Figure 4.2. Regression graph of softening point dataset

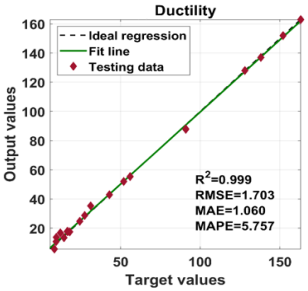

Figure 4.3. Regression graph of ductility dataset

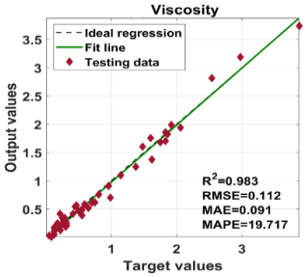

Figure 4.4. Regression graph of viscosity dataset

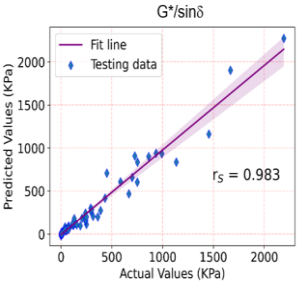

Figure 4.5. Regression graph of G*/sinδ dataset

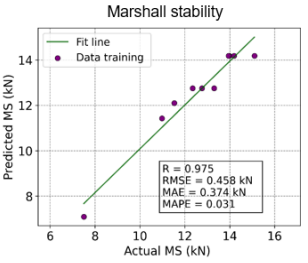

Figure 4.6. Regression graph of MS dataset

Finally, for the convenience of materials engineers and experimenters in selecting input parameters and comparing experimental results with predictions, a Graphical User Interface (GUI) is developed to provide a quick and accurate prediction of the mechanical properties of N_GO and BTN_GO. This is a graphical interface created for interacting with the prediction system, offering a visually intuitive and user-friendly way for users to input data and receive predictions without the need for coding. An illustration of the GUI for predicting the mechanical properties of BTN_GO is shown in Figure 4.10.

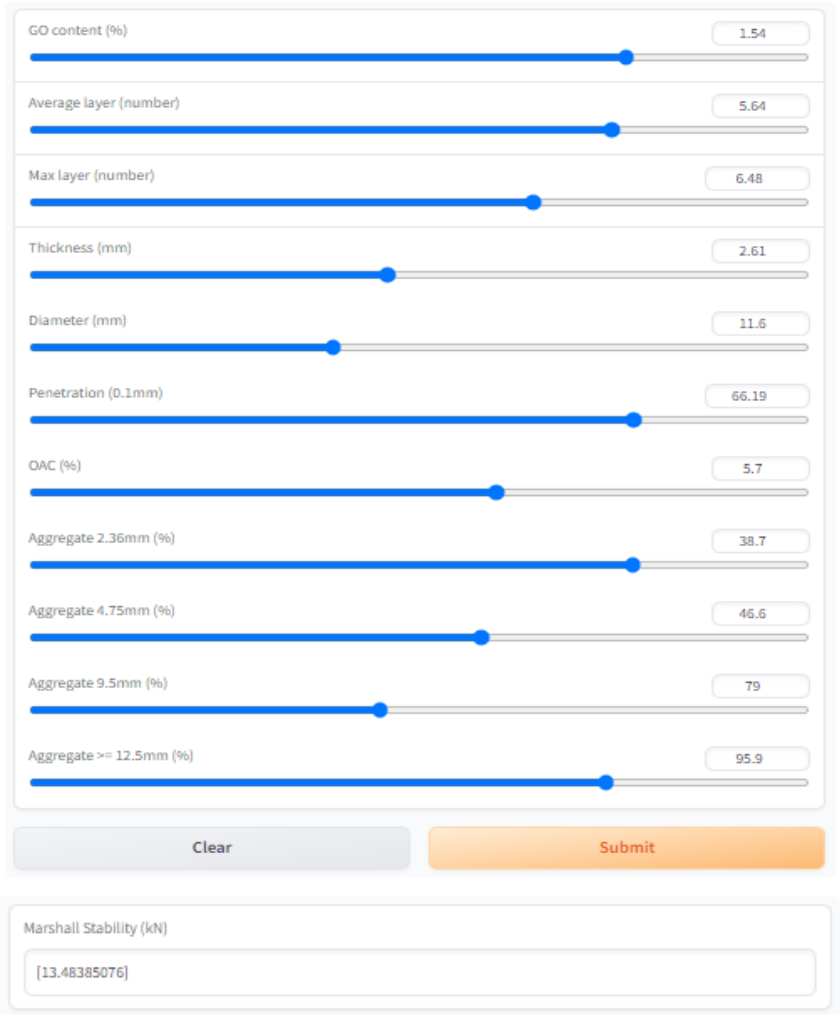

Figure 4.10. GUI for BTN_GO Marshall stability forecast.

4.2. Application of BTN_GO as a surface layer in flexible pavement structures

4.2.1. Typical flexible pavement structures on national highways in Vietnam

In Vietnam, national highways typically use the following typical flexible pavement structure:

- Surface layer: Including 1-2 layers of hot mix asphalt concrete, with or without a functional surface layer, typically having a thickness ranging from 12 to 14 cm.
- Base layer: Includes the above foundation layer and the below foundation layer. The above foundation layer uses Type 1 crushed stone aggregate. The below foundation layer uses Type 1 crushed stone aggregate, Type 2 crushed stone aggregate, graded aggregate, and cement-stabilized sand.

– The bottom layer of the road pavement typically uses selected hill soil or sand with a thickness of 30-50 cm, K ≥ 0.98.

4.2.2. Proposing a pavement structure using BTN_GO

To compare and evaluate BTN_GO when used as a surface layer, the study selected the pavement structure of National Highway 6 as in Table 4.3.

Table 4.3. Pavement structures

No	Material layers	Thickness of layers, cm (KC1)	Thickness of layers, cm (KC2)
1	BTN_60/70	5	-
2	BTN_GO_2%	-	Design
3	BTNC 19	7	7
4	Type 1 crushed stone aggregate	15	15
5	Type 2 crushed stone aggregate	25	25
6	Graded aggregate	30	30
	Total	**82**	**Design**

4.3. Audit of the flexible pavement structure according to TCCS 38:2022/TCĐBVN

The audit results of the 2 flexible pavement structures indicate that, when using BTN_GO_2% layer instead of BTN_60/70 as the surface layer on national highways, the thickness of the surface layer is reduced by 20%, while still ensuring compliance with standard requirements for elasticity, flexural strength, and skid resistance.

4.4. Analyzing the flexible pavement structure using the M-E method

Using the Darwin-ME software with climate data and material layer characteristics to analyze KC1 and KC2 with traffic data. The results of the M-E analysis after 15 years of usage are presented in Table 4.9 to Table 4.11.

Table 4.9. The results analysis according to M-E with N_o (first year) = 686 vehicles/day-night.

No	Evaluation criteria	Target	KC1		KC2	
			Predicted	Evaluate	Predicted	Evaluate
1	Terminal IRI (m/km)	**3,5**	2,28	Pass	2,29	Pass
2	Permanent deformation – total pavement (mm)	**25,0**	20,23	Pass	19,81	Pass
3	AC bottom-up fatigue cracking (m/km)	**25,0**	1,93	Pass	2,10	Pass
4	AC thermal cracking (m/km)	**190**	5,15	Pass	5,15	Pass
5	AC top-down fatigue cracking (m/km)	**380**	220,43	Pass	207,54	Pass
6	Permanent deformation – AC only (mm)	**12,5**	6,26	Pass	5,92	Pass

Table 4.10. The results analysis according to M-E with No (first year) = 1000 vehicles/day-night.

No	Evaluation criteria	Target	KC1		KC2	
			Predicted	Evaluate	Predicted	Evaluate
1	Terminal IRI (m/km)	**3,5**	2,33	Pass	2,34	Pass
2	Permanent deformation – total pavement (mm)	**25,0**	21,96	Pass	20,99	Pass
3	AC bottom-up fatigue cracking (m/km)	**25,0**	2,30	Pass	3,13	Pass
4	AC thermal cracking (m/km)	**190**	5,15	Pass	5,15	Pass
5	AC top-down fatigue cracking (m/km)	**380**	266,22	Pass	251,64	Pass
6	Permanent deformation – AC only (mm)	**12,5**	7,41	Pass	7,01	Pass

Table 4.11. The results analysis according to M-E with No (first year) = 2000 vehicles/day-night.

No	Evaluation criteria	Target	KC1		KC2	
			Predicted	Evaluate	Predicted	Evaluate
1	Terminal IRI (m/km)	**3,5**	2,45	Pass	2,45	Pass
2	Permanent deformation – total pavement (mm)	**25,0**	25,74	Fail	24,86	Pass
3	AC bottom-up fatigue cracking (m/km)	**25,0**	10,31	Pass	17,48	Pass
4	AC thermal cracking (m/km)	**190**	5,15	Pass	5,15	Pass
5	AC top-down fatigue cracking (m/km)	**380**	364,97	Pass	347,67	Pass
6	Permanent deformation – AC only (mm)	**12,5**	10,11	Pass	9,57	Pass

From these results, several observations can be drawn:

- With the same weather conditions, traffic volume, lower layers, and subbase layers, KC2 using BTN_GO as the surface layer experiences a 20% reduction in thickness compared to KC1 while still ensuring equivalent operational characteristics to KC1. Notably, the total rutting depth at the end of the evaluation period for KC2 is lower than KC1 for the studied traffic volumes.
- With N_0 = 2000 vehicles/day-night, KC2 meets all operational characteristics, whereas KC1 fails to meet the total rutting depth requirement for the entire structure.

4.5. Suggesting a manufacturing approach for BTN_GO at the mixing plant

Generally, producing BTN_GO at the mixing plant is quite similar to regular AC production, with the primary difference being in the production of the binding agent. Based on the research results in Chapter 2, the study proposes some key aspects in the production of N_GO and BTN_GO at the mixing plant as follows:

- The N_GO mixing equipment needs to be equipped with blade stirrers arranged offset from each other to create a downward stirring flow towards the bottom of the mixing tank, ensuring the uniform and continuous dispersion of GO particles in the asphalt. The mixing equipment should be equipped with a motor whose power is calculated to achieve a speed of over 2000 rpm for the stirrers. Additionally, the mixing equipment should have a separate inlet for introducing GO, include a heating device, and have temperature sensors to maintain a stable N_GO temperature throughout the mixing process.

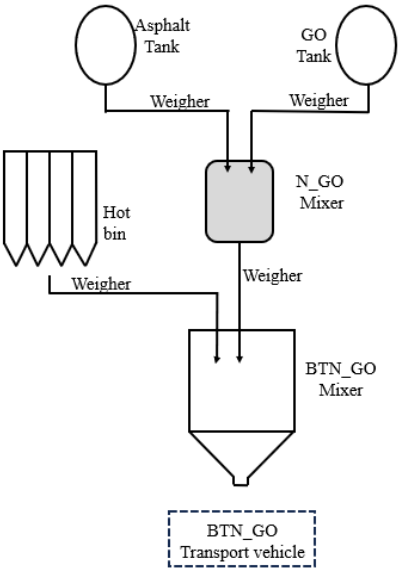

Figure 4.11. Suggesting a manufacturing approach for BTN_GO at the mixing plant.

- GO is supplied by automated equipment with pre-set metering, synchronized with the operation of the mixing plant to form a closed-loop production line.
- At the N_GO mixing equipment, GO is introduced into the pre-heated asphalt at 150°C. The N_GO manufacturing process here follows the mentioned mixing parameters. The timing for discharging the material from the hot bin into the mixing tank must be calculated so that after production, N_GO may be pumped into the mixing tank and mixed with the aggregate for approximately 1 – 2 minutes. During the BTN_GO production process, the mixing temperature is closely controlled (155°C ± 5°C) to ensure the quality of the mixture. The quantity of N_GO needs to be calculated so that one mixing cycle can be used for multiple batches of BTN_GO in a construction shift. Determining the maximum storage time and preservation conditions for N_GO in the mixing equipment and BTN_GO mixture in the mixing tank requires further research.

4.6. Conclusion of Chapter 4

From the research results in Chapter 4, several observations may be made:

- ML algorithms may be applied to develop fast and accurate prediction tools for base properties of N_GO, such as penetration, softening point, viscosity, ductility, G*/sinδ, and Marshall stability of BTN_GO. This provides valuable information and guidance for material engineers in future experiments.
- The design calculation for the flexible pavement structure according to TCCS 38:2022/TCĐBVN shows that it is possible to reduce the thickness of the surface layer using BTN_GO compared to using BTNC 12.5. Specifically, when using BTN_GO_2% instead of BTNC 12.5 for A1-class roads with Eyc ≥ 140 MPa, the thickness of the surface layer will decrease by 20%.
- Analysis of the flexible pavement structure using the M-E method reveals the advantage of rutting resistance in the structure with BTN_GO as the surface layer compared to using BTNC 12.5. The flexible pavement with a BTN_GO_2% surface layer at a thickness of 4 cm can accommodate roads with a higher cumulative heavy vehicle count compared to BTNC 12.5 at 5 cm thickness.
- Through the proposed manufacturing approach for BTN_GO at the mixing plant, the feasibility of BTN_GO production technology in practical settings is demonstrated.

CONCLUSIONS AND RECOMMENDATIONS

I. CONCLUSIONS AND NEW THESIS FINDINGS

1. The proposed content of GO (1 - 2%) by weight of asphalt ensures the dispersion of GO in the asphalt and improves several physical properties of BTN_GO, such as Marshall stability, static elastic modulus, dynamic modulus, splitting tensile strength, and rutting resistance. Additionally, the study also suggests a method for designing the BTN_GO mixture composition and indicates that BTN_GO has a higher mixing and compaction temperature compared to conventional AC from 5 to 8°C.

2. Construction of several regression equations that describe the relationships between the viscosity function, G*/sinδ, Marshall stability, static elastic modulus, splitting tensile strength with the GO content and test temperature. Additionally, research constructed the master curve |E*| for BTN_GO at the reference temperature of 21°C and has made initial indications of the potential applicability of the 2S2P1D viscoelastic model for modeling the dynamic modulus |E*| of BTN_GO.
3. The proposal suggests the application, calculation, simulation, audit and evaluation of a flexible pavement structure with a surface layer using BTN_GO, and initial evidence indicates that this is a promising solution for reducing the thickness and enhancing the operational quality of the pavement structure.
4. Developed prediction tools based on machine learning models for several physical properties of N_GO and BTN_GO. Developed a GUI to assist engineers in using these tools for predicting the physical characteristics of N_GO and BTN_GO without the need for coding.

II. LIMITATIONS

1. The research conducted laboratory experiments and utilized predictive models without the conditions for field experimentation.
2. The research experimented with one type of GO, one type of asphalt, and one type of aggregate from the Sunway quarry in Quoc Oai, Hanoi, which may not be representative of conditions across Vietnam.

III. RECOMMENDATIONS

1. Based on the research results in the laboratory and the analysis of M-E pavement structural parameters, recommend further research on the application of BTN_GO mixtures in the field.
2. Continue assessing the feasibility of BTN_GO when using various types of aggregates, different source materials, asphalt, and different types of GO.

IV. FUTURE RESEARCH DIRECTIONS

1. Research on the storage time of N_GO, BTN_GO at the mixing plant, and the on-site construction technology for BTN_GO.
2. Continue researching the application of the M-E method to analyze the behavior of flexible pavement structures using BTN_GO in different subbase and subgrade layers.
3. Research the use of combining GO with warm mix additives to reduce the mixing and compaction temperatures of AC mixtures, thereby enhancing the improvement in the physical properties of AC.

LIST OF PUBLISHED WORKS

1. **Hoang Thi Huong Giang**, Nguyen Hoang Long, Le Thanh Hai, Le Nho Thien, Vu The Thuan (2021)*, Artificial intelligence approach to predict the penetration and softening point of graphene oxide modified asphalt,* Journal of Science and Transport Technology, No1/2021 pp 41-53.
2. **Hoang Thi Huong Giang**, Le Nho Thien, Vu The Thuan (2022), *Study to predict viscosity of graphene oxide modified bitumen by the enhanced Gradient algorithm,* Transport Journal No 11/2022, pp 46-50.
3. **Huong-Giang Thi Hoang**, Hoang-Long Nguyen, Hai-Bang Ly, Thuy-Anh Nguyen, (2022), *Neural network approach for GO-modified asphalt properties estimation,* Case Studies in Construction Materials, 11/2022 https://doi.org/10.1016/j.cscm.2022.e01617.
4. **Hoang Thi Huong Giang**, Nguyen Hoang Long, Ly Hai Bang (2023), *Study on morphology and chemical composition of the modified asphalt Graphene Oxide using the scanning electron microscope and Fourier variable infrared spectrum,* Transport Journal No 3/2023, pp 76-79.
5. **Hoang Thi Huong Giang**, Nguyen Hoang Long, Ly Hai Bang (2023), *On the physio-mechanical properties of graphene oxide modified asphalt,* Transport Journal No 4/023, pp 59-62.
6. **Huong-Giang Thi Hoang**, Hoang-Long Nguyen, Hai-Bang Ly, Ngoc Hung Tran, (2023)*, Evaluation of the Influence of Graphene Oxide on Asphalt Binder Physical and Rheological Properties,* Journal of Materials: Design and Applications, 6/2023, DOI: 10.1177/14644207231186610).
7. **Huong-Giang Thi Hoang**, Hoang Long Nguyen, Hai-Bang Ly, Hai-Van Thi Mai (2023)*, Application of Extreme Gradient Boosting in Predicting the Viscoelastic Characteristics of Graphene Oxide Modified Asphalt at Medium and High Temperatures,* Frontiers of Structural and Civil Engineering (accepted May, 2023).
8. **Hoang Thi Huong Giang**, Nguyen Hoang Long, Ly Hai Bang (2023), *Experimental Study on Static Elastic Modulus and Flexural Strength of GO-modified Asphalt Concrete,* Transport Journal No 9/2023, pp 117-120